



CHORUS

This is the accepted manuscript made available via CHORUS. The article has been published as:

Systematic approach for simultaneously correcting the band-gap and p-d separation errors of common cation III-V or II-VI binaries in density functional theory calculations within a local density approximation

Jianwei Wang, Yong Zhang, and Lin-Wang Wang

Phys. Rev. B **92**, 045211 — Published 31 July 2015

DOI: [10.1103/PhysRevB.92.045211](https://doi.org/10.1103/PhysRevB.92.045211)

A systematic approach for simultaneously correcting the bandgap and p-d separation errors of common cation III-V or II-VI binaries in density functional theory calculations within a local density approximation

Jianwei Wang¹, Yong Zhang^{1*}, and Lin-Wang Wang²

¹Department of Electrical and Computer Engineering, The University of North Carolina at Charlotte, 9201 University City Boulevard, Charlotte NC 28223, USA

²Materials Sciences Division, Lawrence Berkeley National Laboratory, One Cyclotron Road, Mail Stop 50F, Berkeley, CA 94720, USA

Abstract

We propose a systematic approach that can empirically correct three major errors typically found in the density functional theory (DFT) calculation within a local density approximation (LDA) simultaneously for a set of common cation binary semiconductors, such as III-V compounds – (Ga or In)X with X=N, P, As, Sb, and II-VI compounds (Zn or Cd)X, with X= O, S, Se, Te. By correcting (1) the binary bandgaps at high symmetry points Γ , L, X, (2) the separation of p and d orbital derived valence bands, and (3) conduction band effective masses to experimental values and doing so simultaneously for common cation binaries, the resulting DFT-LDA based quasi first-principles method can be used to predict the electronic structure of complex materials involving multiple binaries with comparable accuracy but much less computational cost than a GW level theory. This approach provides an efficient way to evaluate the electronic structures and other material properties of complex systems much needed for material discovery and design.

PACS number(s): 71.15.-m, 71.15.Dx, 71.15.Mb, 71.20.Nr

* yong.zhang@uncc.edu

I. Introduction

1. The band gap errors in DFT-LDA and their corrections

Various density functional theory (DFT) based modeling methods have become powerful tools to explore the properties of materials.[1,2] DFT methods implemented within a local density approximation (LDA) or generalized gradient approximation (GGA) have been broadly used in ground state calculations for explaining a wide range of ground state phenomena in condensed matter physics, despite its enduring deficiency in describing exchange and correlation energies and the lack of derivative discontinuity in their exchange-correlation functional.[1] The best known consequence of this deficiency is perhaps that LDA tends to underestimate the band gap in semiconductors and insulators, compared with experimental results.[3] It also affects valence band properties, such as the energy separation of the valence bands derived from p orbitals and highly localized d orbitals.[4] Many different alternative methods have been developed to address this problem,[3,5-21] mostly famously a many-body perturbation GW method which is capable of reproducing the experimental bandgaps of common semiconductors to within 0.1 – 0.3 eV.[18-21] However, GW is computationally very expensive, and sometimes suffers from the conduction band cutoff convergence problem.[22] Although it is now possible to use a GW method to calculate systems up to one hundred atoms,[23] it is still difficult to calculate systems much larger than that, e.g., a thousand atom nanostructure. It is thus beneficial to have DFT methods which only require the LDA level computational effort, but can predict the electronic structure accurately. For many practical problems, we encounter new systems that are heterostructures built upon two or more well-studied binaries, for instance, in the form of an alloy or a superlattice that involves a structural unit much larger than a GW method can calculate. Examples may include quaternary alloys GaAsSbN for applications in multi-junction solar cell,

IR detection and emission,[24,25] highly lattice mismatched ZnO-ZnSe core-shell nanowires for PV application.[26] For somewhat structurally simpler but large structures, for instance, binary quantum dots and wires or ternary alloys, some DFT-LDA based techniques incorporating atomistic level empirical corrections to the atomic pseudopotentials have been shown able to yield rather satisfactory results to selected properties ranging from structural properties (in the DFT-LDA level) to electronic and optical properties (after applying the empirical correction, DFT-LDA-C).[27-34] In certain cases, a DFT-LDA-C method can often offer very good results for the electronic structure, with accuracy comparable to that of optical spectroscopy (typically in the order of 10 meV).[35-38] Besides the electronic structure, this type approach has also been shown to yield significantly better results in calculating the ground state properties (e.g., binary formation energy).[39] However, it remains impractical to calculate more complex structures that involve more than two binaries and correct LDA errors in more than just bandgap (see more discussions later). Thus, a systematic correction to the DFT method can provide a powerful tool for accurate material simulations and material discovery.

2. Empirical methods and comparison with DFT

The empirical methods, especially a k·p method,[40] often show some advantages over the first-principles methods in accuracy when using them to describe the bulk electronic structure, when the necessary input parameters are available experimentally. Based on the k·p perturbation theory, a limited set of parameters (for example, Luttinger parameters γ_1 , γ_2 , γ_3 and electronic effective mass m^*) are used to fit the experimentally determined dispersions of the conduction bands and valence bands. Such fitting usually can give very accurate descriptions of the experimentally derived bulk band structures near high symmetry points of Brillouin zoon (BZ). More significantly, the fitting parameters can often be used for predicting heterostructures

consisting of the relevant bulk materials, for instance, a superlattice. The success of the k·p theory lies in that the symmetry of the band structure is correctly described by a set of symmetry operators, where the relevant coefficients can be determined empirically. These coefficients are otherwise difficult to obtain with high accuracy through direct first-principles calculations. Of course, a k·p based theory has its major limitation in dealing with the situation where the atomistic scale structure modification becomes important. The success of various non-self-consistent atomistic methods is in fact in the same spirit, although implicitly, in particular in a tight-binding approach.[41] An empirical pseudopotential method (EPM) can actually predict the electronic structure of a semiconductor alloy with an accuracy in the order of 10 meV, when the atomic pseudopotentials for binaries are accurately obtained.[42] However, such a non-self-consistent method is incapable of predicting the structure of the material and dealing with inter-atomic charge transfer. Therefore, it is highly desirable to have a DFT-LDA-C method that incorporates empirical corrections in the atomistic level to mitigate the LDA bandgap errors. As a matter of fact, there have been a number of approaches proposed in the literature along this line, including one that has been used by some of us in recent years,[27] that is, after performing the self-consistent calculation, empirical corrections to the s, p, and d components of atomistic pseudopotentials are introduced to fit the major bandgaps of the binaries to the experimental values. This approach has been shown to work very well, often with few meV accuracy in determining the impurity levels and alloy bandgaps.[35-37] However, in the past, the fitting was typically done case by case for two binaries with a common cation, for instance, GaP and GaN or GaAs and GaN, where the correction to Ga pseudopotentials were different for the two pairs. Thus, for each new heterostructure binary pair, a new fitting will be needed. Furthermore, to correct the LDA error in effective mass, a different set of the parameters, which might not

necessarily be able to also yield satisfactory bandgaps, would be required.[28] This situation limits the applicability of this method to more complex structures, not to mention non-common cation structures. In addition, the LDA error in the valence band p-d separation was not corrected, which could affect the accuracy in the description of the valence band and related impurity or defect states.

In this work, we develop a systematic approach that allows us to generate a single set of s, p, and d atomistic pseudopotential corrections for a given cation, e.g., Zn, that works near equally well with different anions of the same group: O, S, Se, Te, that can simultaneously correct bandgaps of the most important critical points (Γ , L, and X) and the valence band p-d separation. This method is also applicable and usually sufficient to treat a non-common cation system, because the corrections for the anions can be realized by taking weighted average based on their coordination number with different cations, as done in the EPM.[42] With this approach, one may be able to predict the electronic structure with the GW level accuracy or even better for any superstructures involving, for instance, (Zn or Cd)X (X = O, S, Se, Te) with only the computational effort of LDA. Note that simultaneous fitting multiple binaries not only allows us to deal with more complex structures but also applies more constrain to the parameters and reduces the ambiguity and potentially improves the transferability to other materials. Furthermore, once the energy levels of the critical points are correctly determined, we expect that the correct dispersion relations in the whole BZ should also follow naturally, for instance, the effective masses. The approach is also applicable to most commonly encountered III-V binaries: (Ga or In)X (X = N, P, As, Sb), with the possibility to include more elements. In a nutshell, our approach is in the same spirit of the k·p theory but at an atomistic level, because the electronic states of different high symmetry \mathbf{k} points are related by the symmetry operations of the system

and can be determined by a small set of parameters that can be more conveniently derived experimentally. In the meantime, the conventional DFT-LDA or GGA can be used for computing the ground state properties of the system.

II. Computational methods

1. DFT-LDA calculations

A plane wave pseudopotential code PEtot [43] is used for the binary band structure calculation in LDA with norm conservation pseudopotentials. The exchange-correlation contribution is accounted for by means of Perdew and Zunger's parametrization of the calculations by Ceperley and Alder.[44] The d electrons are included as valence electrons for cation atoms. The special k points are generated using an $8 \times 8 \times 8$ mesh, which generates 60 special k points in the first BZ. The spin-orbit coupling is included using Escan code.[45] The experimental lattice constants are used. The kinetic energy cut-off has been tested and chosen to be 60 Ry. The semiconductors considered here are all in the zinc blende (ZB) structure, even though some may prefer to crystallize in wurtzite phase in the normal growth condition.

In our approach, a local correction term is added to each of the s, p, d nonlocal pseudopotentials to fit the band gaps at high symmetry points of the BZ (e.g., Γ , X and L points in ZB structure).[27] In the past, we only fit the band gaps involving these states: Γ_{8v} , Γ_{1c} , X_{1c} , X_{3c} and L_{1c} of the ZB structure, while keeping the LDA valence band maximum (VBM) fixed (no net change). However, a major portion of the band gap error in LDA can be due to the p-d valence band separation E_{p-d} being too small, which causes too strong p-d repulsion that pushes up the VBM. This effect is well-known to be critically important for getting the correct band gap for some binary (e.g., ZnO), as well as in describing the band offset between two binaries. Thus,

in this work, we introduce a correction to the cation d orbital to adjust the p-d separation to match the experimentally measured values.

2. Procedures for making band gap corrections

The method described here is still a post-treatment in order to produce accurate band structure. A self-consistent calculation is performed first to generate the charge density and local potential.

There are six s, p, d atomic orbitals available for a given binary in fitting. If we want to fit, for instance, ZnX (X = O, S, Se, Te) with the same set of Zn orbitals, there will be less adjustable parameters. It is important to have the general insight of how different orbitals affect energy levels at special k points. We first briefly review the impact of each orbital to the energy levels of interested high symmetry points. Figure 1 shows the calculated band structure of ZnTe in LDA, together with the projections of the s, p, d density of states (DOS). The d bands (one triplet $d_{3/2}$ and one doublet state $d_{1/2}$ without spin-orbit coupling, or two doublet and one singlet state with spin-orbit coupling) are located very close to each other and form a band, which is referred to as d band. The width of d band is usually in the range of several hundred of meV. The center of d band is used to calculate the p-d separation E_{p-d} where the p energy level is taken from the top of valence band.

Compared the energy levels with the projected DOS, the d component of Zn in the DOS is far great than others at the center of the d band. This suggests that the d band mainly comes from the d orbital of Zn. There are some components coming from other orbitals near the center of the d band, for instance, the second major component is the p orbital of Te, which reflects the p-d coupling. This information suggests the first step of the action should be adjusting the d orbital of Zn atom to make calculated E_{p-d} matching the corresponding experimental value.

Figure 2 plots δE_{p-d} vs. $\delta V(\text{Zn}_d)$ for the four binaries, where $\delta E_{p-d} = E_{p-d}(\text{Cal.}) - E_{p-d}(\text{Expt.})$ is the deviation of E_{p-d} relative to its experimental value, and $\delta V(\text{Zn}_d)$ is the amplitude of local potential added to the d-component of the Zn pseudopotential. It can be seen from Fig. 2 that δE_{p-d} can be tuned from -2.81 eV to 1.47 eV when $\delta V(\text{Zn}_d)$ varies from 0.0 to -0.3. We note that the $\delta V(\text{Zn}_d)$ value that yields the best correction (i.e., $\delta E_{p-d} = 0$) only varies slightly from one binary to the other, as shown in the inset of Fig. 2, which are -0.194, -0.198, -0.188, and -0.200, respectively, for ZnO, ZnS, ZnSe, and ZnTe. Therefore, we can achieve very good fitting of E_{p-d} for all ZnX (X=O, S, Se and Te) by simply taking the average value of $\delta V(\text{Zn}_d) = -0.195$. The corresponding errors of E_{p-d} are merely 12 meV, 45 meV, 105 meV and 75 meV for ZnO, ZnS, ZnSe, and ZnTe, respectively. The largest error is 105 meV for ZnSe, which is negligible compared to E_{p-d} of 9.20 eV. It is interesting and important to find that a common value $\delta V(\text{Zn}_d) = -0.195$ can simultaneously correct E_{p-d} for all the binaries with deviations comparable to the uncertainty of the experimental data. This adjustment of p-d separation is very similar to the treatment of p-d coupling in LDA-1/2 method, [46] where a trimmed self-energy potential derived from cation d states is added to get an improved bandgap.

After the $\delta V(\text{Zn}_d)$ correction is applied, the VBM values of ZnX (X=O, S, Se, Te) are lowered by 550, 284, 227, 162 meV, respectively. Here the lowering is respect to the core levels (i.e., the VBM becomes closer to the core levels). On one hand, the E_{p-d} error contributes significantly to the LDA errors in the bandgaps; on the other hand, the dependence of the VBM error on anion type also significantly affects the band offsets among these common cation binaries. Once this step is done, no further adjustment will be made to this parameter in the future steps of correcting other bandgaps, and this adjusted VBM will be viewed as the correct and final one which should be kept with as little net change as possible after applying other

subsequent correction steps. This new VBM is used as the reference energy level for the targeted conduction band energy levels at special k points according to their experimental values or GW calculation results when reliable experimental data are not available. When the spin-orbit coupling is included, a one third of spin-orbit coupling Δ_{SO} should be added to the above mentioned VBM.

How the other energy levels are determined by the different orbitals is complicated because of the presence of different couplings, such as s-p and p-d coupling? We continue to use ZnTe as an example to examine the effects of each individual pseudopotential component. Figure 3 shows the effects of changing all the six components on five energy levels: VBM and conduction Γ_{1c} , X_{1c} , L_{1c} , and X_{3c} . The VBM state mainly comes from the Te p orbital, but is also affected significantly by the Zn d and p orbital, and slightly by Te d orbital, which is confirmed by Fig. 3(e), 3(c), 3(b), and 3(f). The CBM at different k points exhibit different dependences on the atomic orbitals: Γ_{1c} is affected by both $\delta V(\text{Te}_s)$ and $\delta V(\text{Zn}_s)$; X_{1c} by $\delta V(\text{Zn}_p)$, $\delta V(\text{Zn}_d)$, $\delta V(\text{Te}_s)$, and $\delta V(\text{Te}_d)$, but not by $\delta V(\text{Zn}_s)$ and $\delta V(\text{Te}_p)$; L_{1c} is affected by all six components, although only very weakly by $\delta V(\text{Zn}_d)$ and $\delta V(\text{Te}_p)$; and X_{3c} depends on $\delta V(\text{Zn}_s)$, $\delta V(\text{Zn}_d)$, $\delta V(\text{Te}_p)$, and $\delta V(\text{Te}_d)$, but not by $\delta V(\text{Zn}_p)$ and $\delta V(\text{Te}_s)$. Note that the fitting of E_{p-d} has some minor effects on the conduction band, specifically, on X_{1c} , L_{1c} , and X_{3c} , as shown in Fig. 3(c).

Our general goal here is to adjust the four conduction band states Γ_{1c} , X_{1c} , L_{1c} , and X_{3c} to obtain correct bandgaps with respect to VBM without causing further net change in VBM, using the five remaining pseudo-potential components. One way to do it would be performing a least square fitting using the curves produced in Fig. 3. However, we have developed an interactive three-step procedure that usually works better. First, we note that the effects of $\delta V(\text{Te}_d)$ on X_{1c}

and X_{3c} and $\delta V(\text{Zn}_p)$ on X_{1c} tend to saturate after certain values, but the corrections are still not enough. So we adopt a value close to the saturation point for each of these two variables. Second, since the previous step has changed VBM due to $\delta V(\text{Zn}_p)$, we use $\delta V(\text{Te}_p)$ to bring it back. Third, we use the two left over parameters $\delta V(\text{Zn}_s)$ and $\delta V(\text{Te}_s)$ to get Γ_{1c} and X_{1c} to the targeted values, and in the meantime the separation of X_{3c} and X_{1c} close to be the targeted value as well. Usually, the experimental value for the X_{3c} is less well known and its value is also less critical to the properties of interest, we play more weights on Γ_{1c} and X_{1c} . L_{1c} is not explicitly included in these steps, but typically turns out to be fairly close to the targeted value, which can be taken as an indicator for the success of this procedure. We note that the exact order of these steps is not critical.

The procedure described above allows us to perform LDA corrections for the whole set of binaries with a common cation, in this case, ZnX ($X = \text{O}, \text{S}, \text{Se}, \text{Te}$). The same correction parameters for the three components of the Zn pseudopotential are shared by all the Zn based binaries. We also apply this approach to Cd based II-VI compounds, and Ga and In based III-V compounds. The corrected results are described in the following section, and all the fitting parameters are given in Appendix. The original (generated by the PEtot package [43]) and corrected pseudopotentials are available on our group website [47] or can be provided upon request.

III. Results and Discussion

Listed in Table I are the LDA-corrected results of spin-orbit coupling, p-d separation, and energy levels of Γ_{1c} , X_{1c} , X_{3c} and L_{1c} for group II-VI semiconductors with Zn and Cd as cation. Table II contains the same results for group III-V semiconductors with Ga and In as cation. Overall, these corrected values are at least as good if not better than what have been achieved

before either by applying other empirical correction schemes or using GW, in particular, done simultaneously for multiple common-cation compounds.

The corrected Γ_{1c} bandgaps are typically within a few meV of the targeted values for all binaries. For an indirect bandgap material like GaP with its CBM at the X point, the deviation is only 63 meV from its experimental value. The comparisons between the raw LDA, LDA-corrected and experimental or targeted bandgaps for Γ_{1c} , X_{1c} and L_{1c} are compiled in Figure 4. The electronic band structures are plotted in Figure 5 for selected compounds GaAs, InSb, ZnTe, and CdTe.

Besides the bandgaps at the special k points, we further test the ability of the correction scheme for generating accurate dispersion curves, specifically effective mass. The electron effective masses along the [001] direction are calculated and compared with available experimental or calculation results, tabulated in Table III. The agreements are remarkably well. The ability to also yield accurate effective mass further affirms the success and reliability of this correction scheme, because it is resting on sound physics based on the internal symmetry connection among different special k points.

Although the corrections were applied to the ZB structure, the modified pseudopotentials can be used in predicting other crystal structures. For instance, we have calculated ZnO with wurtzite structure, and found the band gap to be 3.52 eV which is consistent with the GW calculation and experimental results ~ 3.60 eV.[48] The same correction parameters can be used for more complex structures, such as superlattices and alloys. We have recently applied this method to the band structures of InAs/GaSb type II superlattices with small bandgaps of 10 – 100 meV, where the LDA calculation typically yield negative bandgaps. Very good agreements with experimental results were achieved after applying the correction.[38] Based on the success

of applying this approach to the InAs/GaSb superlattice, this method should be able to give more accurate band offsets than the straight DFT. However, it is beyond the scope of this work to explicitly extracting the band offset values for these materials, which on its own would be a significant effort.[49]

IV. Conclusions

In conclusion, we have developed a systemic approach to correct the band gap errors in DFT-LDA calculations. A reliable and easy to follow procedure is prescribed and demonstrated with great success for producing correct band structures for III-V and II-VI compounds, including the bandgaps at most important critical points, p-d band separation in the valence band, and the conduction band effective mass. As a method offering atomistic level corrections to the LDA results for ZB structure, the transferability to other related structures have been tested yielding very good results. The ability to simultaneously correct multiple common cation binaries with the same correction parameters for the cation makes it very useful for studying complex structures with multiple anions and cations. In the future, more extensive testing will be performed for computing other band structure parameters, such as deformation potentials, and various material properties. This approach is expected to be as accurate as GW, sometimes even better, for many practical applications but without the demand for large computational resources.

Acknowledgements

Work at UNCC was supported by U.S. ARO/MURI Program (Grant No. Army W911NF-10-1-0524 and monitored by Dr. William Clark). Y. Zhang acknowledge support of Bissell Distinguished Professorship. L.W. Wang's work is supported by the Director, Office of Science, Basic Energy Science/Materials Science and Engineering Division of the U.S. Department of

Energy (DOE) under the contract No. DE-AC02-05CH11231 through the Materials Theory program. This work used computational resource at NERSC.

References

- [1] R. M. Martin, *Electronic Structure: Basic Theory and Practical Methods* (Cambridge University Press, 2008).
- [2] W. Kohn and L. J. Sham, *Phys. Rev.* **140**, A1133 (1965).
- [3] J. P. Perdew and A. Zunger, *Phys. Rev. B* **23**, 5048 (1981).
- [4] S. H. Wei and A. Zunger, *Phys. Rev. B* **37**, 8958 (1988).
- [5] I. A. Vladimir, F. Aryasetiawan, and A. I. Lichtenstein, *J. Phys.: Condens. Matter* **9**, 767 (1997).
- [6] R. W. Godby, M. Schlüter, and L. J. Sham, *Phys. Rev. B* **37**, 10159 (1988).
- [7] R. Asahi, W. Mannstadt, and A. J. Freeman, *Phys. Rev. B* **59**, 7486 (1999).
- [8] A. Seidl, A. Görling, P. Vogl, J. A. Majewski, and M. Levy, *Phys. Rev. B* **53**, 3764 (1996).
- [9] M. Städele, M. Moukara, J. A. Majewski, P. Vogl, and A. Görling, *Phys. Rev. B* **59**, 10031 (1999).
- [10] A. Qteish, A. I. Al-Sharif, M. Fuchs, M. Scheffler, S. Boeck, and J. Neugebauer, *Phys. Rev. B* **72**, 155317 (2005).
- [11] F. Tran and P. Blaha, *Phys. Rev. Lett.* **102**, 226401 (2009).
- [12] Y.-S. Kim, M. Marsman, G. Kresse, F. Tran, and P. Blaha, *Phys. Rev. B* **82**, 205212 (2010).
- [13] J. A. Camargo-Martínez and R. Baquero, *Phys. Rev. B* **86**, 195106 (2012).
- [14] D. C. Langreth and M. J. Mehl, *Phys. Rev. B* **28**, 1809 (1983).
- [15] J. P. Perdew, K. Burke, and M. Ernzerhof, *Phys. Rev. Lett.* **77**, 3865 (1996).
- [16] J. Heyd, G. E. Scuseria, and M. Ernzerhof, *J. Chem. Phys.* **118**, 8207 (2003).
- [17] J. Heyd, J. E. Peralta, G. E. Scuseria, and R. L. Martin, *J. Chem. Phys.* **123**, 174101 (2005).
- [18] M. S. Hybertsen and S. G. Louie, *Phys. Rev. B* **34**, 5390 (1986).
- [19] F. Aryasetiawan and O. Gunnarsson, *Rep. Prog. Phys.* **61**, 237 (1998).
- [20] K. A. Johnson and N. W. Ashcroft, *Phys. Rev. B* **58**, 15548 (1998).
- [21] M. Shishkin, M. Marsman, and G. Kresse, *Phys. Rev. Lett.* **99**, 246403 (2007).
- [22] M. L. Tiago, S. Ismail-Beigi, and S. G. Louie, *Phys. Rev. B* **69**, 125212 (2004).
- [23] J. Deslippe, G. Samsonidze, D. A. Strubbe, M. Jain, M. L. Cohen, and S. G. Louie, *Comput. Phys. Commun.* **183**, 1269 (2012).
- [24] G. Ungaro, G. Le Roux, R. Teissier, and J. C. Harmand, *Electron. Lett.* **35**, 1246 (1999).
- [25] T. W. Kim, K. Forghani, L. J. Mawst, T. F. Kuech, S. D. LaLumondiere, Y. Sin, W. T. Lotshaw, and S. C. Moss, *J. Cryst. Growth.* **393**, 70 (2014).
- [26] Z. Wu *et al.*, *J. Mater. Chem.* **21**, 6020 (2011).
- [27] L.-W. Wang, *Appl. Phys. Lett.* **78**, 1565 (2001).
- [28] J. Li and L.-W. Wang, *Phys. Rev. B* **72**, 125325 (2005).
- [29] J. Li and S.-H. Wei, *Phys. Rev. B* **73**, 041201 (2006).
- [30] D. Segev, A. Janotti, and C. G. Van de Walle, *Phys. Rev. B* **75**, 035201 (2007).
- [31] S.-H. Wei and A. Zunger, *Phys. Rev. B* **57**, 8983 (1998).
- [32] J. Schrier, D. O. Demchenko, L. W. Wang, and A. P. Alivisatos, *Nano Lett.* **7**, 2377 (2007).
- [33] Y. Zhang, Wang, and A. Mascarenhas, *Nano Lett.* **7**, 1264 (2007).
- [34] N. E. Christensen, *Phys. Rev. B* **30**, 5753 (1984).
- [35] Y. Zhang, B. Fluegel, M. C. Hanna, A. Mascarenhas, L.-W. Wang, Y. J. Wang, and X. Wei, *Phys. Rev. B* **68**, 075210 (2003).
- [36] Y. Zhang, A. Mascarenhas, and L. W. Wang, *Phys. Rev. B* **74**, 041201 (2006).
- [37] Y. Zhang, A. Mascarenhas, and L. W. Wang, *Phys. Rev. B* **71**, 155201 (2005).
- [38] J. Wang and Y. Zhang, *J. Appl. Phys.* **116**, 214301 (2014).
- [39] V. Stevanovic, S. Lany, X. Zhang, and A. Zunger, *Phys. Rev. B* **85**, 115104 (2012).
- [40] L. C. Lew Yan Voon and M. Willatzen, *The k - p Method: Electronic Properties of Semiconductors* (Springer, Berlin, 2009).

- [41] P. Vogl, H. P. Hjalmarson, and J. D. Dow, *J. Phys. Chem. Solids* **44**, 365 (1983).
- [42] Y. Zhang, A. Mascarenhas, and L.-W. Wang, *Phys. Rev. B* **63**, 201312 (2001).
- [43] <http://cmsn.lbl.gov/html/PEtot/PEtot.html>.
- [44] D. M. Ceperley and B. J. Alder, *Phys. Rev. Lett.* **45**, 566 (1980).
- [45] <http://cmsn.lbl.gov/html/EScan/DOE-nano/pescan.htm>.
- [46] L. G. Ferreira, M. Marques, and L. K. Teles, *Phys. Rev. B* **78**, 125116 (2008).
- [47] <http://coefs.uncc.edu/yzhang47/>.
- [48] B.-C. Shih, Y. Xue, P. Zhang, M. L. Cohen, and S. G. Louie, *Phys. Rev. Lett.* **105**, 146401 (2010).
- [49] Y.-H. Li, A. Walsh, S. Chen, W.-J. Yin, J.-H. Yang, J. Li, J. L. F. Da Silva, X. G. Gong, and S.-H. Wei, *Appl. Phys. Lett.* **94**, 212109 (2009).
- [50] M. Oshikiri and F. Aryasetiawan, *Phys. Rev. B* **60**, 10754 (1999).
- [51] O. Zakharov, A. Rubio, X. Blase, M. L. Cohen, and S. G. Louie, *Phys. Rev. B* **50**, 10780 (1994).
- [52] S. Z. Karazhanov, P. Ravindran, A. Kjekshus, H. Fjellvåg, U. Grossner, and B. G. Svensson, *J. Appl. Phys.* **100**, 043709 (2006).
- [53] P. Carrier and S.-H. Wei, *Phys. Rev. B* **70**, 035212 (2004).
- [54] R. A. Powell, W. E. Spicer, and J. C. McMenamin, *Phys. Rev. Lett.* **27**, 97 (1971).
- [55] S. H. Wei and A. Zunger, *Appl. Phys. Lett.* **69**, 2719 (1996).
- [56] Y. Zhang, A. Mascarenhas, and L. W. Wang, *Phys. Rev. Lett.* **101**, 036403 (2008).
- [57] D. A. H. Mace, D. C. Rogers, K. J. Monserrat, J. N. Tohill, and S. T. Davey, *Semicond. Sci. Technol.* **3**, 597 (1988).
- [58] W. F. Boyle and R. J. Sladek, *Phys. Rev. B* **11**, 2933 (1975).
- [59] I. Vurgaftman, J. R. Meyer, and L. R. Ram-Mohan, *J. Appl. Phys.* **89**, 5815 (2001).
- [60] D. E. Aspnes, C. G. Olson, and D. W. Lynch, *Phys. Rev. B* **14**, 4450 (1976).
- [61] K. P. Ghatak, S. Bhattacharya, S. Bhowmik, R. Benedictus, and S. Choudhury, *J. Appl. Phys.* **103**, 034303 (2008).
- [62] C. Persson and A. Zunger, *Phys. Rev. B* **68**, 073205 (2003).
- [63] L. Ley, R. A. Pollak, F. R. McFeely, S. P. Kowalczyk, and D. A. Shirley, *Phys. Rev. B* **9**, 600 (1974).
- [64] G. Ramírez-Flores, H. Navarro-Contreras, A. Lastras-Martínez, R. C. Powell, and J. E. Greene, *Phys. Rev. B* **50**, 8433 (1994).
- [65] S. E. Stokowski and D. D. Sell, *Phys. Rev. B* **5**, 1636 (1972).
- [66] A. Rubio, J. L. Corkill, M. L. Cohen, E. L. Shirley, and S. G. Louie, *Phys. Rev. B* **48**, 11810 (1993).
- [67] J.-M. Jancu, R. Scholz, F. Beltram, and F. Bassani, *Phys. Rev. B* **57**, 6493 (1998).
- [68] R. W. Godby, M. Schlüter, and L. J. Sham, *Phys. Rev. B* **35**, 4170 (1987).
- [69] S.-H. Wei and A. Zunger, *Phys. Rev. B* **39**, 3279 (1989).
- [70] X. Zhu and S. G. Louie, *Phys. Rev. B* **43**, 14142 (1991).
- [71] D. M. Brad and L. C. Marvin, *J. Phys.: Condens. Matter* **25**, 105503 (2013).
- [72] O. Madelung, *Semiconductors: Data Handbook* (Springer Berlin Heidelberg, 2004).

TABLE I. LDA-corrected spin-orbit coupling Δ_{SO} , p-d separation E_{p-d} , and energy levels at special k points Γ_{1c} , X_{1c} , X_{3c} , and L_{1c} for ZnX (X= O, S, Se, and Te) and CdX (X=S, Se, and Te). Numbers in parenthesis (), squiggly brackets {}, and square brackets [] denote the experimental values, quasiparticle (GW) calculation results, and original LDA calculation results without the corrections, respectively.

	a (Å)	Δ_{SO} (eV)	E_{p-d} (eV)	Γ_{1c} (eV)	X_{1c} (eV)	X_{3c} (eV)	L_{1c} (eV)
ZnO	4.620 ^a	-0.005 (-0.004 [†]) [-0.032]	7.513 (7.5 ^e) [5.381]	3.394 {3.394 ^g } [0.521]	8.316 {8.199 ^g } [5.176]	10.384 {10.998 ^g } [8.416]	7.782 {8.449 ^g } [5.131]
ZnS	5.409 ^b	0.067 (0.067 ^c) [-0.054]	8.985 (9.03 ^f) [6.560]	3.800 (3.80 ^b) [1.751]	5.182 {5.14 ^b } [3.183]	5.460 {6.03 ^b } [3.868]	5.156 {5.28 ^b } [3.006]
ZnSe	5.668 ^b	0.404 (0.400 ^c) [0.348]	9.305 (9.20 ^f) [6.787]	2.82 (2.82 ^b) [0.960]	4.428 {4.41 ^b } [2.704]	4.452 {5.01 ^b } [3.191]	4.153 {4.14 ^b } [2.234]
ZnTe	6.089 ^b	0.986 (0.970 ^c) [0.902]	9.765 (9.84 ^f) [7.323]	2.398 (2.39 ^b) [0.609]	3.364 {3.47 ^b } [1.877]	3.670 {3.53 ^b } [1.943]	3.188 {3.07 ^b } [1.273]
CdS	5.818 ^b	0.051 (0.067 ^d) [0.051]	9.737 (9.64 ^f) [7.776]	2.552 (2.55 ^b) [0.832]	5.196 {5.08 ^b } [3.277]	5.725 {6.17 ^b } [4.141]	4.675 {4.82 ^b } [2.720]
CdSe	6.052 ^b	0.417 (0.416 ^d) [0.400]	10.027 (10.04 ^f) [8.125]	1.901 (1.90 ^b) [0.270]	4.419 {4.37 ^b } [2.785]	4.673 {5.20 ^b } [3.476]	3.788 {3.87 ^b } [2.064]
CdTe	6.480 ^b	0.926 (0.920 ^d) [0.879]	10.402 (10.49 ^f) [8.570]	1.603 (1.60 ^b) [0.140]	3.511 {3.46 ^b } [2.144]	3.658 {3.64 ^b } [2.280]	2.993 {2.84 ^b } [1.299]

^a Reference [50]

^b Reference [51]

^c Reference [52]

^d Reference [53]

^e Reference [54]

^f Reference [4]

^g Reference [48]

[†] Δ_{SO} (wurtzite)

TABLE II. LDA-corrected spin-orbit coupling Δ_{SO} , p-d separation E_{p-d} , and energy levels at special k points Γ_{1c} , X_{1c} , X_{3c} , and L_{1c} for GaX (X= N, P, As and Sb) and InX (X=P, As and Sb). Numbers in parenthesis (), squiggly brackets {}, and square brackets [] denote the experimental values, quasiparticle (GW) calculation results, and original LDA calculation results without the corrections, respectively.

	a (Å)	Δ_{SO} (eV)	E_{p-d} (eV)	Γ_{1c} (eV)	X_{1c} (eV)	X_{3c} (eV)	L_{1c} (eV)
GaN	4.50 ^a	0.009 0.015 ^a [0.016]	17.441 (17.0 ^b) [13.810]	3.305 (3.302 ⁱ) [1.678]	4.703 {4.7 ^l } [3.308]	7.807 {8.4 ^l } [6.525]	6.304 {6.2 ^l } [4.469]
GaP	5.409 ^b	0.075 (0.080 ^e) [0.102]	18.446 (18.55 ⁱ) [14.711]	2.871 (2.869 ^k) [1.456]	2.413 (2.350 ^m) [1.474]	2.425 (2.75 ^{m,q}) [1.644]	2.706 (2.64 ^q) [1.404]

GaAs	5.6533 ^c	0.345 (0.340 ^e) [0.336]	18.657 (18.9 ⁱ) [14.976]	1.520 (1.519 ^e) [0.346]	1.989 (1.98 ^{n,p}) [1.352]	2.099 (2.30 ^p) [1.480]	1.869 (1.81 ^p) [0.828]
GaSb	6.089 ^d	0.765 (0.752 ^f) [0.663]	18.890 (19.0 ⁱ) [15.284]	0.814 (0.8102 ^f) [-0.348]	1.778 (1.66 ^p) [0.624]	1.259 (1.43 ^p) [0.943]	1.092 (1.09 ^p) [0.068]
InP	5.818 ^d	0.060 (0.108 ^e) [0.121]	16.902 (16.80 ⁱ) [14.372]	1.439 (1.4236 ^e) [0.352]	2.440 {2.58 ^q } [1.568]	2.639 {3.08 ^q } [2.062]	2.200 {2.03 ^q } [1.200]
InAs	6.052 ^c	0.387 (0.380 ^g) [0.418]	17.015 (17.09 ⁱ) [14.097]	0.419 (0.418 ^g) [-0.051]	2.100 {2.01 ^q } [1.405]	2.430 {2.50 ^q } [1.887]	1.604 (1.55 ^q) [0.720]
InSb	6.480 ^e	0.839 (0.810 ^g) [0.803]	17.262 (17.29 ⁱ) [14.908]	0.237 (0.2352 ^{e,g}) [-0.728]	1.378 {1.50 ^q } [0.996]	2.005 {1.57 ^q } [1.001]	1.018 (0.89 ^f) [0.102]

^a Reference [55]	^b Reference [56]	^c Reference [57]	^d Reference [58]
^e Reference [59]	^f Reference [60]	^g Reference [61]	^h Reference [62]
ⁱ Reference [63]	^j Reference [64]	^k Reference [65]	^l Reference [66]
^m Reference [67]	ⁿ Reference [68]	^p Reference [69]	^q Reference [70]
^r Reference [71]			

TABLE III. Effective mass of electrons for III-V and II-VI semiconductors (in unit of the electron free mass m_0) calculated by original LDA, LDA+C method, are compared with their available experimental values.

	LDA	LDA+C	Expt.		LDA	LDA+C	Expt.
GaN	0.171	0.167	0.20 ^a	ZnO	0.131	0.219	
GaP	0.104	0.112	0.13 ^a	ZnS	0.074	0.161	0.184 ^b
GaAs	0.053	0.066	0.067 ^a	ZnSe	0.090	0.113	0.130 ^b
GaSb	0.015	0.045	0.039 ^a	ZnTe	0.068	0.102	0.130 ^b
InP	0.059	0.081	0.0795 ^a	CdS	0.109	0.137	
InAs	0.016	0.023	0.026 ^a	CdSe	0.065	0.099	0.12 ^c
InSb	0.087	0.015	0.0135 ^a	CdTe	0.066	0.085	0.094 ^c

^a Reference [59]	^b Reference [52]	^c Reference [72]
-----------------------------	-----------------------------	-----------------------------

Figure captions:

Figure 1. The electronic structure (left) and partial density of states (right) for zinc-blende ZnTe from a DFT-LDA calculation without spin-orbit coupling.

Figure 2. The deviation of the p-d separation δE_{p-d} , $\delta E_{p-d} = E_{p-d}(\text{cal.}) - E_{p-d}(\text{expt.})$, vs. $\delta V(\text{Zn}_d)$ for ZnO, ZnS, ZnSe and ZnTe. The inset shows an enlarged view for the $\delta V(\text{Zn}_d)$ region where δE_{p-d} approaching zero.

Figure 3. Shifts of energy levels (VBM, Γ_{1c} , X_{1c} , X_{3c} , and L_{1c}) vs. fitting parameters of six orbitals (s, p, and d orbitals of Zn atom and Te atom).

Figure 4. A comparison of experimental band gaps with those calculated with LDA and LDA+C methods.

Figure 5. Band structures of GaAs, InSb, ZnSe, and CdTe.

Figure 1

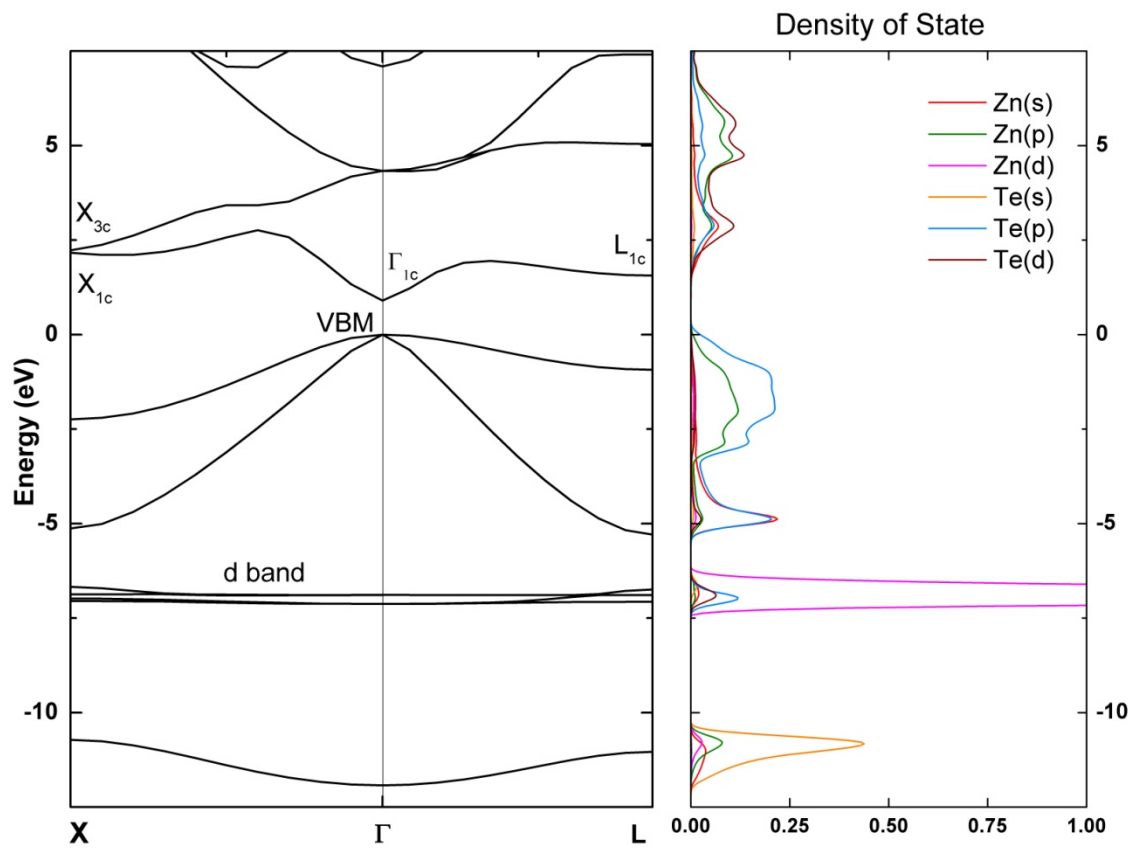


Figure 2

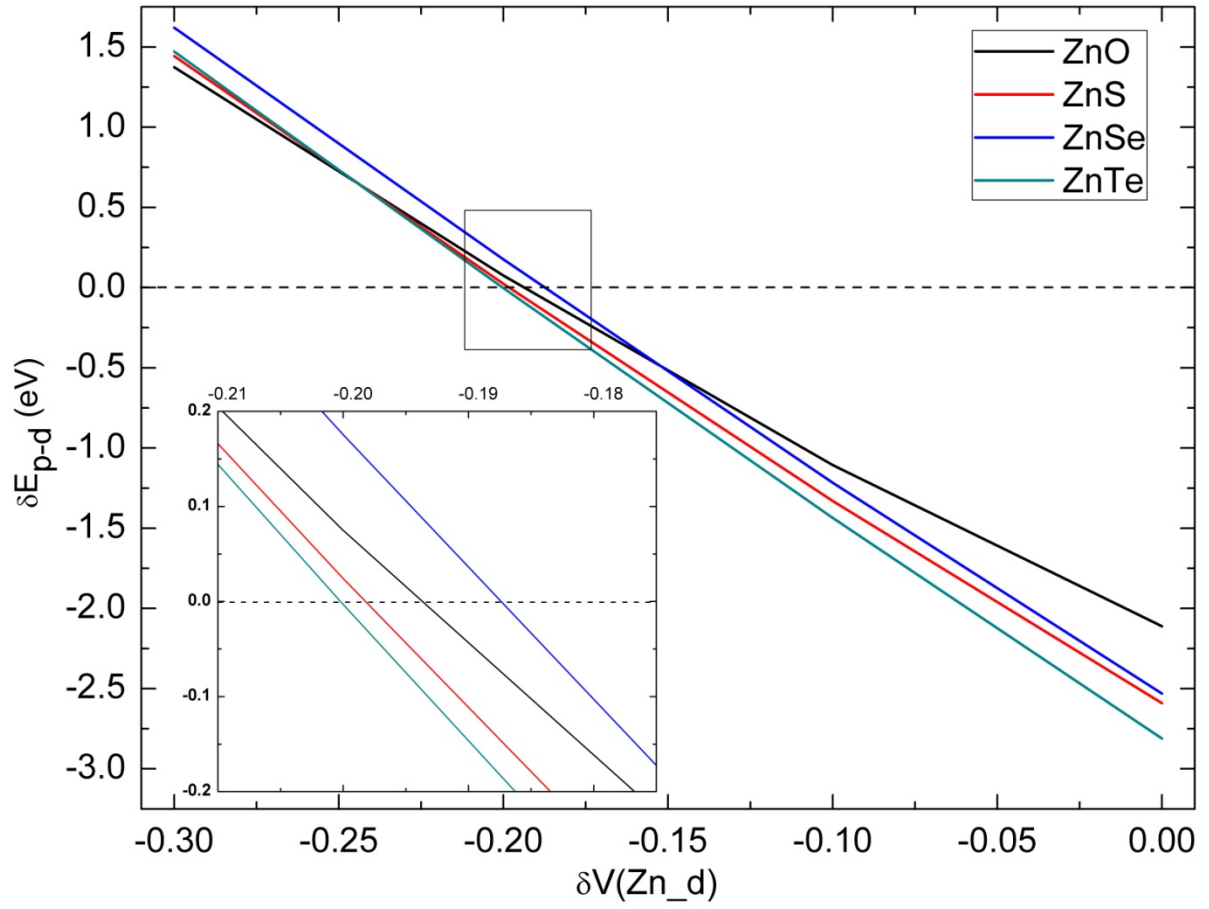


Figure 3

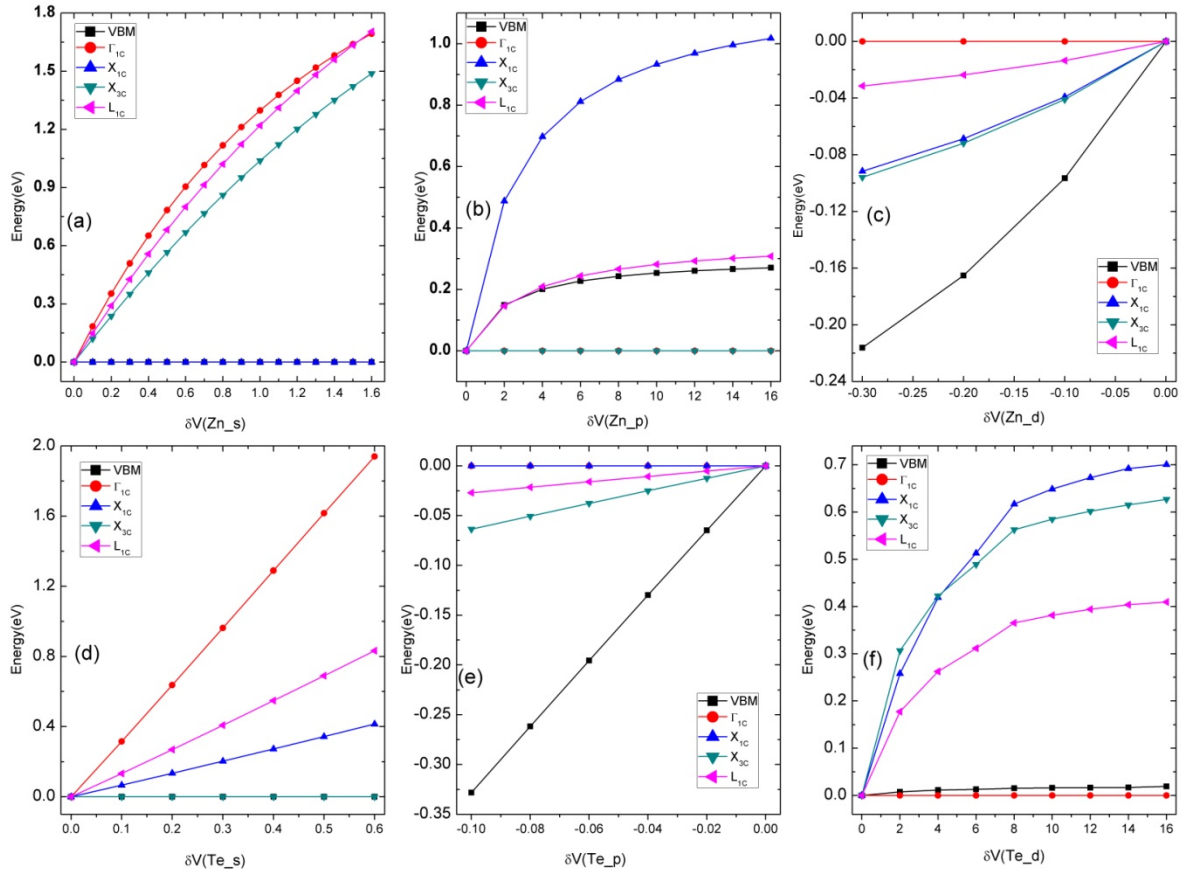


Figure 4

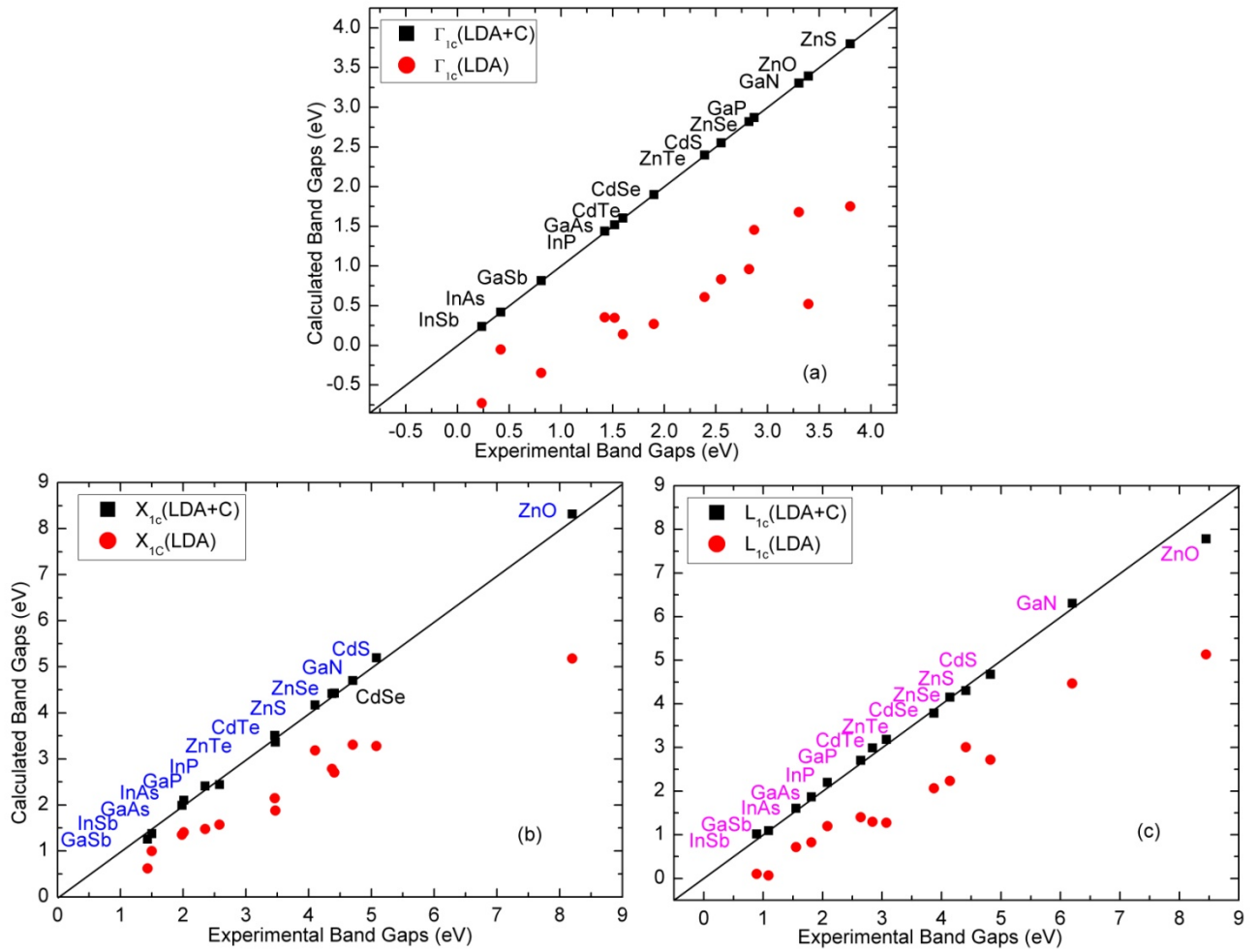
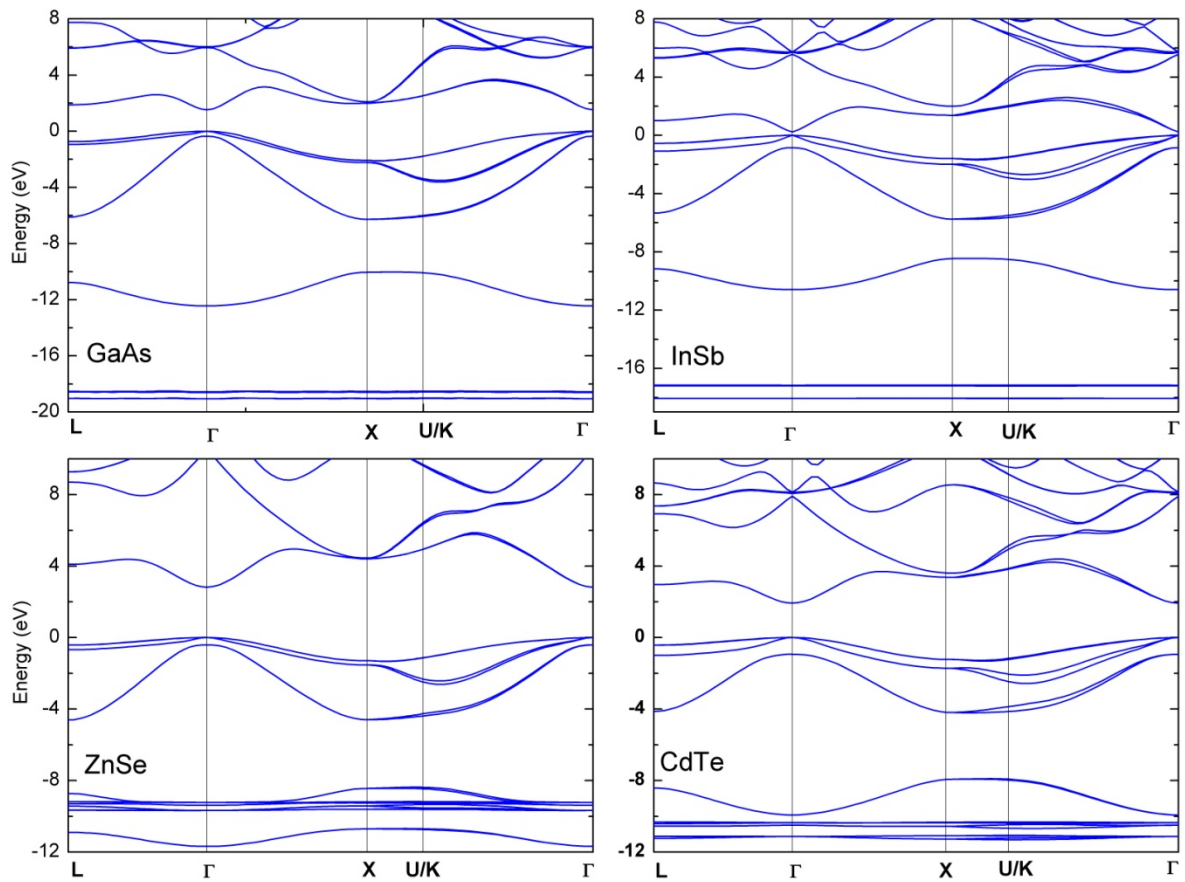


Figure 5



Appendix

Table A-I. List of cutoff radius (in unit of Bohr radius) for pseudopotentials

	r_c		r_c		r_c
Zn_s	2.30	Zn_p	2.30	Zn_d	2.30
O_s	1.45	O_p	1.45	O_d	1.00
S_s	1.70	S_p	1.70	S_d	1.70
Se_s	1.90	Se_p	1.90	Se_d	1.90
Te_s	2.60	Te_p	2.60	Te_d	2.60
Cd_s	2.65	Cd_p	2.65	Cd_d	2.65
Ga_s	2.10	Ga_p	2.10	Ga_d	2.10
In_s	2.90	In_p	2.90	In_d	2.90
N_s	1.50	N_p	1.50	N_d	0.00
P_s	1.95	P_p	1.95	P_d	1.95
As_s	2.10	As_p	2.40	As_d	3.00
Sb_s	2.60	Sb_p	2.60	Sb_d	2.60

Table A-II. Fitting parameters for ZnX

Zn_s	0.500	Zn_p	10.0	Zn_d	-0.19502525
O_s	0.652555	O_p	-0.0273929	O_d	10.0
S_s	0.640480	S_p	-0.1008	S_d	5.0
Se_s	0.568804	Se_p	-0.114591	Se_d	10.0
Te_s	0.269504	Te_p	-0.072394	Te_d	22.0

Table A-III. Fitting parameters for CdX

Cd_s	0.450	Cd_p	7.00	Cd_d	-0.172982
S_s	0.621348	S_p	-0.08192	S_d	22.0
Se_s	0.574695	Se_p	-0.094994	Se_d	12.0
Te_s	0.345548	Te_p	-0.060212	Te_d	4.0

Table A-IV. Fitting parameters for GaX

Ga_s	0.60	Ga_p	3.482	Ga_d	-0.252373
N_s	0.250114	N_p	-0.0348319	N_d	6.0
P_s	0.174723	P_p	-0.129255	P_d	1.29255
As_s	0.0649773	As_p	-0.0862555	As_d	0.0
Sb_s	-0.141989	Sb_p	-0.002094	Sb_d	2.0

Table A-V. Fitting parameters for InX

In_s	0.20	In_p	2.0	In_d	-0.172582
P_s	0.196927	P_p	-0.119467	P_d	0.0
As_s	0.107101	As_p	-0.0833195	As_d	-0.50
Sb_s	0.0880463	Sb_p	-0.130506	Sb_d	1.0